Chemistry & Biology
Article

Design of a Heterobivalent Ligand to Inhibit IgE Clustering on Mast Cells

Michael W. Handlogten,[1] Tanyel Kiziltepe,[1,3] Demetri T. Moustakas,[4] and Başar Bilgiçer[1,2,3,*]
[1]Department of Chemical and Biomolecular Engineering
[2]Department of Chemistry and Biochemistry
[3]Advanced Diagnostics and Therapeutics
University of Notre Dame, Notre Dame, IN 46556, USA
[4]Department of Chemistry and Chemical Biology, Harvard University, Cambridge, MA 02138, USA
*Correspondence: bbilgicer@nd.edu
DOI 10.1016/j.chembiol.2011.06.012

SUMMARY

We describe the design, synthesis, and characterization of a heterobivalent ligand (HBL) system that competitively inhibits allergen binding to mast cell bound IgE antibody, thereby inhibiting mast cell degranulation. HBLs are composed of a hapten conjugated to a nucleotide analog allowing simultaneous targeting of the antigen-binding site as well the "unconventional nucleotide binding site" on IgE Fab domains. Simultaneous bivalent binding to both sites provides HBLs with over 100-fold enhancement both in avidity for IgE^{DNP} (K_d = 0.33 μM) and in inhibition of allergen binding to IgE^{DNP} (IC_{50} = 0.45 μM) than the monovalent hapten (K_d^{mono} = 41 μM; IC_{50}^{mono} = 55.4 μM, respectively). In cellular assays, HBL2 effectively inhibits mast cell degranulation (IC_{50} = 15 μM), whereas no inhibition is detected by the monovalent hapten. In conclusion, this study establishes the use of multivalency in a novel HBL design to inhibit mast cell degranulation.

INTRODUCTION

Allergy results from an abnormal response of the adaptive immune system directed against noninfectious environmental substances (allergens) (Galli et al., 2008). Mast cells are the major effector cells that mediate allergic responses. Cross-linking of IgE bound to its high-affinity receptor (FcεRI) on the surface with multivalent allergens results in activation due to aggregation of FcεRIs (Metzger, 1992; Turner and Kinet, 1999). This FcεRI-dependent activation of mast cells results in degranulation, which causes secretion of preformed mediators that are stored in cytoplasmic granules, such as vasoactive amines, neutral proteases, proteoglycans, cytokines, and chemokines (Blank and Rivera, 2006).

Specific inhibition of allergic response requires recognition of the allergen binding IgE; therefore, in studies aiming to achieve such selectivity, haptenic derivatives of allergens have been used. In earlier examples, monovalent haptens have been tested for their ability to selectively inhibit IgE cross-linking by multivalent allergens. This approach, however, requires excessive amounts of monovalent hapten to accomplish any inhibition due to the short falling of monovalent binding affinity compared to multivalent allergen avidity. (A hapten is a small monovalent molecule that binds to an antibody but does not stimulate an immune response.) Therefore, this approach has only resulted in limited success (Guéant et al., 1999; Mertes et al., 2008; Richter et al., 1981; Romano and Ventura, 2008; Salvin, 1971). Ordinarily, use of multivalent versions of haptens results in cross-linking of mast cell bound IgEs, initiating an allergic response through the same mechanism as the natural allergen, however, this effect has been shown to be reversed with the use of long linkers (>5 nm) (Baird et al., 2003; Kane et al., 1988).

In this study, we incorporate multivalency in a novel design to inhibit mast cell degranulation by inhibiting allergen binding to IgE. Multivalent interactions provide higher affinity (termed avidity) than individual binding moieties: this arises from the combined synergistic binding affinity of the components (Kiessling et al., 2006; Mammen et al., 1998). Examples in literature demonstrate that bivalent binding, as in the case of antibodies, can strengthen avidity of interactions by up to six orders of magnitude over monovalent binding (Bilgiçer et al., 2007, 2009; Carlson et al., 2007; Wang et al., 2000; Wieslander et al., 1990). Literature also has several reports that demonstrate importance and applications of multivalency in biological and synthetic systems (Kane, 2006; Kitov et al., 2000; Rao et al., 2000; Tong et al., 2009; Vance et al., 2008; Wolfenden and Cloninger, 2005; Yi et al., 2007; Zhang et al., 2004). In our approach, we have designed heterobivalent ligands of a haptenic derivative to simultaneously target the antigen binding site on IgE, as well as the "unconventional nucleotide binding site," located proximal to the antigen binding site on the Fab domain of IgE (Rajagopalan et al., 1996). We predicted that the simultaneous bivalent binding to both sites would provide heterobivalent ligands with enhanced avidity and selectivity for IgE, necessary for competitive inhibition of allergen IgE binding (Figure 1).

The heterobivalent ligands have three moieties to consider in design: the nucleotide analog, the hapten, and the linker. The nucleotide-binding site was first described by Rajagopalan et al. (1996). The authors describe the site to be in the "conserved" region of the variable domain of murine immunoglobulin Gs (Figure 2A), and they speculated that this site was likely conserved in all isotypes of immunoglobulins. They also reported that this site accommodated binding of one ATP (adenine)

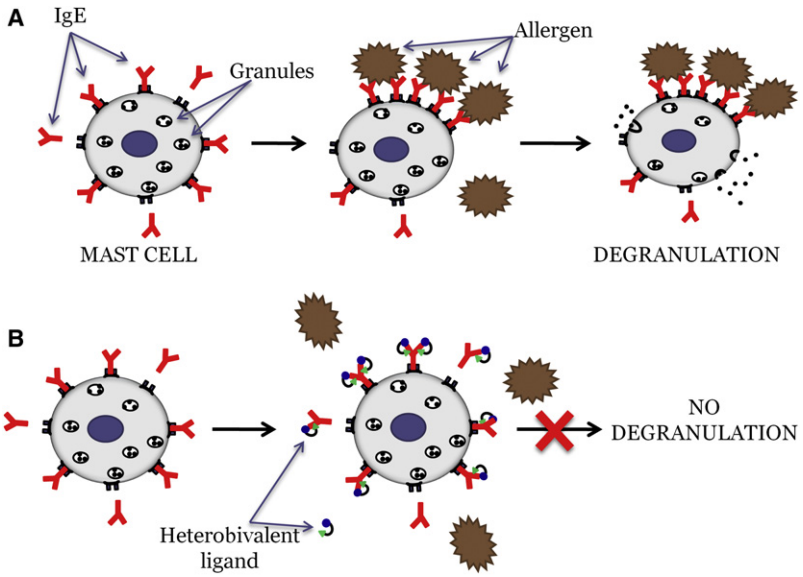

Figure 1. Inhibition of Mast Cell Degranulation Using Heterobivalent Ligands

(A) Degranulation occurs when a multivalent antigen binds to multiple IgE antibodies on the surface of mast cells causing cross-linking of the IgE receptor, FcεRI, initiating a signaling cascade that results in the release of histamine and other inflammatory and cytotoxic molecules.

(B) Heterobivalent ligands were engineered to simultaneously bind to the antigen binding region and the nucleotide binding pocket on the Fab domains of an IgE. Due to the enhanced avidity of the heterobivalent ligand, it inhibits the binding of the allergen to the surface bound IgE thus preventing degranulation.

molecule to each Fab with a dissociation constant of ~50 μM. To find a more potent nucleotide analog, we performed a computational screening for appropriate candidates, as described in the Experimental Procedures. We selected nitrofuran (NF)/IgE^{DNP} as our antibody/hapten pair, because IgE^{DNP} is used in well-established model systems where allergic responses are studied (Andrews et al., 2007; Oliver et al., 1994). Once these two moieties were selected, we experimentally screened for the linkers with the desired length, flexibility, and chemistry that aided the best binding.

Our studies establish that with the appropriate linker between the two binding moieties, heterobivalent ligands are able to inhibit allergen binding to IgE at >100-fold lower concentrations than the corresponding monovalent hapten. Engineered heterobivalent ligands based on haptenic derivatives of allergens are therefore able to competitively and selectively inhibit allergen binding to IgEs, in turn inhibiting FcεRI clustering and allergic response. Furthermore, the concept presented in this study establishes usefulness for the nucleotide-binding site on immunoglobulins in inhibiting mast cell degranulation, a previously ignored binding site. We describe proof of principle studies for inhibition of allergic responses by use of heterobivalent ligands.

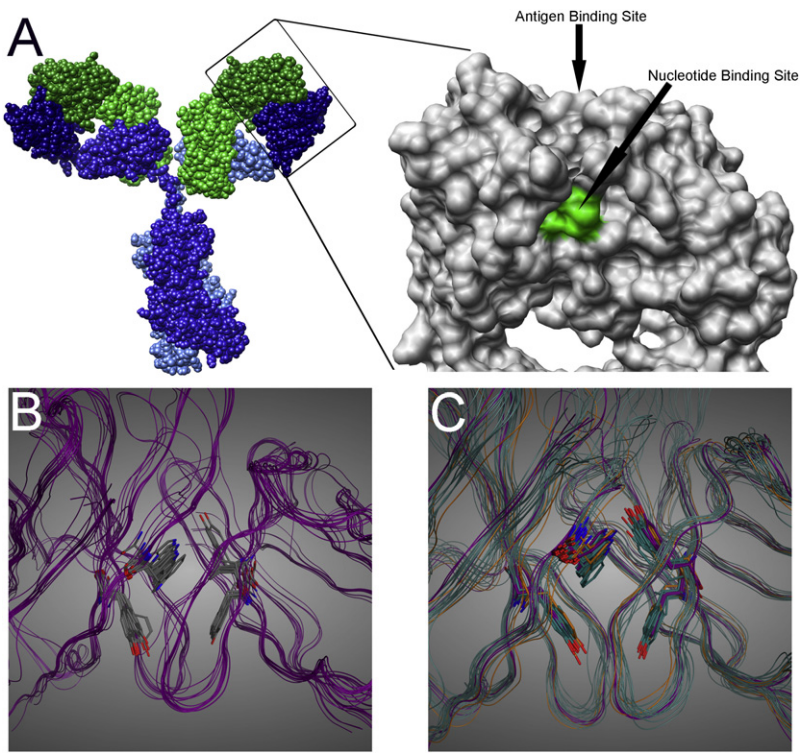

Figure 2. Location of the Conserved Nucleotide Binding Site in Antibodies

(A) Representative crystal structure of an IgG antibody (PDB 1IGY). Enlarged view of the Fab region of an immunoglobulin with the antigen and nucleotide binding sites labeled.

(B) Backbone alignment of nine IgE antibody structures with the residues that make up the nucleotide binding pocket shown. PDB numbers for the IgE crystal structures: 2VXQ, 2R56, 1OAQ, 1OAR, 1OAU, 1OAX, 1OAY, 1OAZ, and 1OCW.

(C) Backbone alignment of 18 IgG, IgM, and IgE antibody structures with the residues of the nucleotide binding pocket shown. The invariability of the side chain configurations demonstrate that the nucleotide binding pocket is conserved through these various isotypes of antibodies. PDB numbers for the overlaid crystal structures are 1DN0, 1DQL, 2VXQ, 2R56, 1AE6, 1BBD, 1DBB, 1F58, 1GGB, 1HIM, 1IGF, 1IKF, 1MAM, 1MRD, 1NCD, 1Q9W, 1UZ8, and 2IFF.

RESULTS

The Nucleotide Binding Site on Immunoglobulins

The design of heterobivalent ligands described in this study is based on targeting the nucleotide-binding site in IgE antibodies. First, we confirmed that this site is conserved in a variety of immunoglobulins through molecular modeling. To this end, we performed a least-squares root-mean-square deviation superposition of all Fab domain crystal structures of IgE antibodies (total of 9) available in the RSCB Protein Data Bank (Figure 2B). The overlaid structures show the framework region of the nucleotide binding region to be conserved throughout all IgE antibodies. Additionally, because the nucleotide binding site is likely conserved throughout all immunoglobulin isotypes, we overlaid >260 immunoglobulin crystal structures, including IgE, IgG, and IgM demonstrating that residues of the nucleotide binding region are conserved throughout antibody isotypes. As a representative group, in Figure 2C, we show 18 overlaid crystal structures from a collection of IgE, IgG, and IgM isotypes. Specifically, our analysis revealed that four residues, namely two tyrosine residues from the light chain, one tyrosine, and one tryptophan residue from the heavy chain, are conserved in all immunoglobulin isotypes. Furthermore, the conformations of these side chains are also highly conserved in the available immunoglobulin crystal structures (Figure 2).

Next, we determined an appropriate nucleotide analog. According to previously published results, adenine binds to the nucleotide binding site with a K_d of 50 μM (Rajagopalan et al., 1996). For our purposes, the nucleotide binding site targeting moiety (nucleotide analog) must have the right affinity for this site, such that, efficient binding to IgE antibodies is obtained only when it is conjugated to the hapten. A nucleotide analog with weak binding affinity would not result in the required enhancement in avidity of heterobivalent ligand binding. On the other hand, extremely strong affinity would also not yield the desired outcome, because, the nucleotide analog would bind nonspecifically to all immunoglobulin isotypes regardless of the presence or absence of the hapten as the nucleotide binding site is conserved in all antibody isotypes. Given that only a small minority of the antibodies in human plasma are IgEs, other isotypes would act as a competitive sink for such heterobivalent ligands. With these considerations in mind, we hypothesized that a K_d of ~1 μM (quite common for interactions between immune components) would provide the optimal binding properties for the nucleotide analog—much tighter than that of ATP. Therefore by use of computational methods (virtual screening method), we examined a small library of commercially available molecules similar to adenine to identify the analog that would potentially have higher binding affinities to the nucleotide binding site (CAS numbers of the compounds screened were as follows: 58944-73-3, 52562-50-2, 133-32-4, 575-85-9, 14490-05-2, 2338-71-8, 4771-50-0.). Results of this screen predicted that indole-3-butyric acid (IBA) would bind with the highest affinity of the compounds screened. The binding affinity of IBA to the IgE^{DNP} was determined experimentally using the fluorescence quenching method. The IBA derivative that was used in this titration, ML2, was synthesized by conjugating IBA to 5-((2-aminoethyl)amino)naphthalene-1-sulfonic acid (EDANS). The EDANS excitation wavelength overlaps with the tryptophan emission wavelength; therefore this system provided us a method to determine IBA binding to IgE^{DNP} by fluorescence quenching. These experiments yielded a binding constant of 4.5 ± 0.6 μM for ML2 and IgE^{DNP}. Our control experiments established that EDANS does not bind IgE^{DNP} (see Figure S1 available online).

Model IgE/Hapten System

The dinitrophenyl/anti-DNP IgE (DNP/IgE^{DNP}) is the most commonly used hapten/antibody system to study allergic responses. The drawback of this system is that DNP binds to IgE^{DNP} with an atypically high monovalent binding affinity (James et al., 2003). Therefore, we decided to use a variant of the DNP/IgE^{DNP} system: the NF/IgE^{DNP} pair. Based on crystal structure analysis, NF was not expected to cause steric problems such as occupying the nucleotide-binding site as would be the case for DNP (James et al., 2003). With these design tenets in mind, the NF/IgE^{DNP} pair was chosen as an appropriate model system to carry out the proof of principle experiments described in this study. We used a fluorescence quenching method for the NF hapten system to determine binding constants to IgE^{DNP}. The absorbance profile of NF overlaps with the fluorescence emission of the tryptophans in IgE^{DNP}. This overlap provides a straightforward spectroscopic method to directly measure the extent of association between NF and IgE^{DNP}. Upon binding of NF to IgE^{DNP}, fluorescence from the IgE^{DNP} tryptophan residues is quenched, and using this method, we determined that NF binds to IgE^{DNP} with a binding constant (K_d) of 41 ± 3 μM (ML1 in Table 1; see Experimental Procedures for detailed equations).

Optimization of Heterobivalent Ligands and Thermodynamic Analysis of IgE-Heterobivalent Ligand Interactions

Next we synthesized the heterobivalent ligands of NF-IBA with various linker molecules using solid phase synthesis. We determined the binding constants of heterobivalent ligands listed in Table 1 to IgE^{DNP} using fluorescence quenching. As can be seen from the measured binding constants, linker length and flexibility play a very important role. The heterobivalent ligand that had the lowest K_d (0.33 ± 0.07 μM) was HBL2, where the linker was six repeating units of ethylene glycol (EG_6). Ethylene glycol linkers have high water solubility (lowest hydrophobicity) and good flexibility. The next three tight binders were also ethylene glycol linkers with slightly shorter (EG_5), slightly longer (EG_8), and much longer (EG_{24}) lengths with K_d 0.79 ± 0.06 μM (HBL1), 0.55 ± 0.03 μM (HBL3), and 0.96 ± 0.05 μM (HBL4) respectively, establishing the importance of proper linker length. Increase in the hydrophobicity of the linker by using ε-linked lysine residues resulted in diminution of binding avidities as seen for molecules HBL5 and HBL6, whose K_d values were determined to be 30 ± 3 μM and 15 ± 1 μM. Furthermore, increasing the rigidity of the linker by incorporating 4-carboxy piperidine in the linkers did not yield favorable results. Specifically, increasing the number of 4-carboxy piperidine from 1 to 4 (HBL7-10), yielded K_d 1.6 ± 0.2 μM, 1.9 ± 0.2 μM, 2.0 ± 0.2 μM, and 15 ± 1 μM. In summary, the most effective heterobivalent ligand was HBL2, synthesized using EG_6 as the linker. Representative binding curves of HBL2 to IgE^{DNP} are shown in Figure 3A. This molecule shows a 124-fold enhancement over

Table 1. Structures of the ML and HBL Ligands with Their Corresponding Extended Length and Apparent Affinities for IgE^{DNP}

Molecule	Structure	Length (Å)	K_d (μM)
ML1	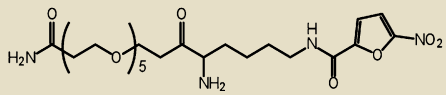	N/A	41 ± 3
ML2	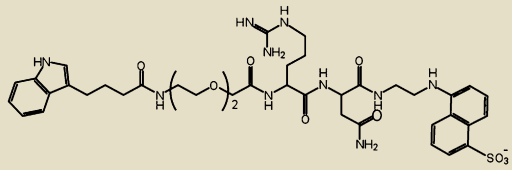	N/A	4.5 ± 0.6
HBL1 (n = 5)	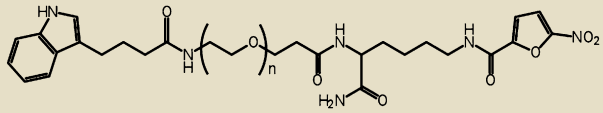	25	0.79 ± 0.06
HBL2 (n = 6)		28.5	0.33 ± 0.07
HBL3 (n = 8)		34	0.55 ± 0.03
HBL4 (n = 24)		92	0.96 ± 0.05
HBL5 (n = 2)	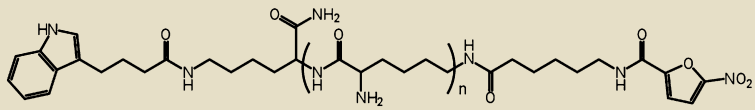	26.7	30 ± 3
HBL6 (n = 3)		34	15 ± 1
HBL7	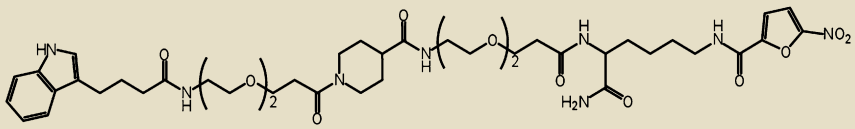	32.2	1.6 ± 0.2
HBL8	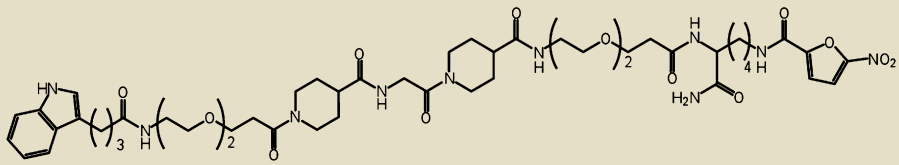	33.1	1.9 ± 0.2
HBL9	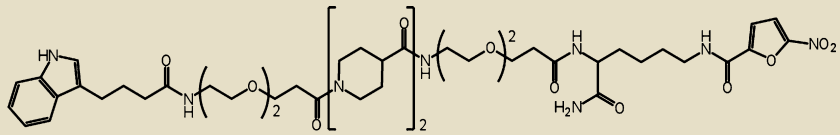	36.8	2.0 ± 0.2
HBL10	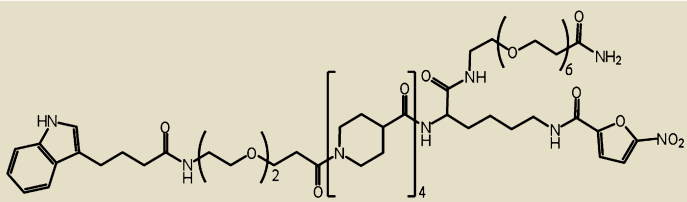	29.5	15 ± 1

HBL, heterobivalent; ML, monovalent; N/A, not applicable. The linkers for HBL1-4 have polyethylene glycol linkers of different length, HBL5-6 have ε-linked lysine residues that are more hydrophobic than ethylene glycol, and HBL7-10 incorporate rigid carboxy piperidine residues.

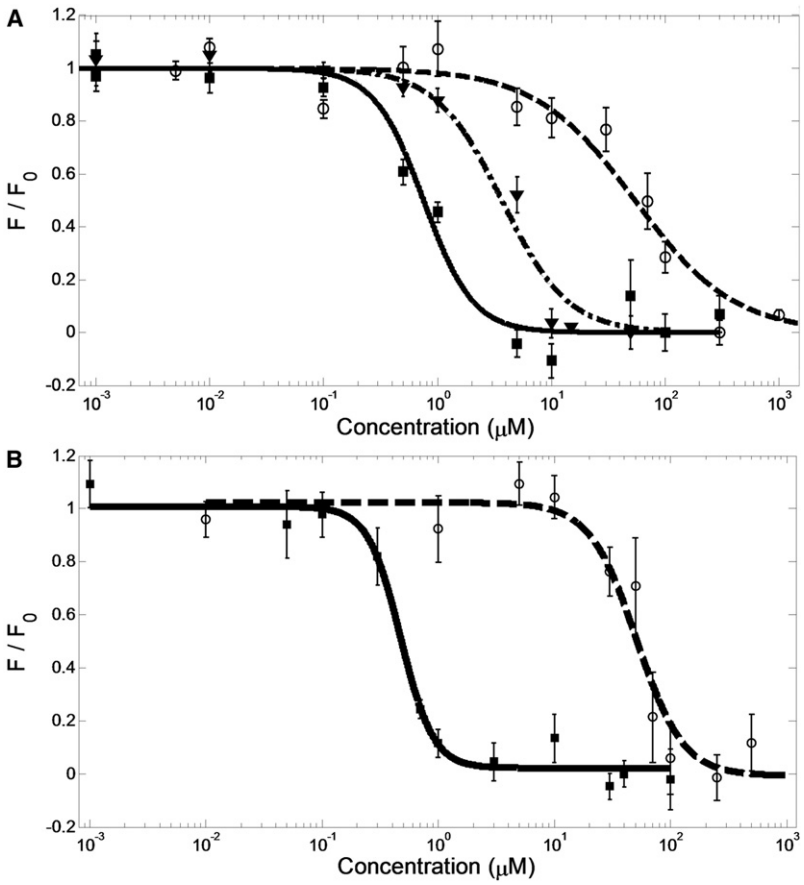

Figure 3. HBL2 Binds to IgE^{DNP} with 124-Fold Affinity over ML1

(A) Representative binding curves for HBL2 (■), monovalent NF (ML1: ○), and monovalent IBA (ML2: ▼) binding to IgE^{DNP}. Binding was observed by monitoring fluorescence quenching of tryptophan as described in the Experimental Procedures section. Values for the various molecules: K_d^{HBL2} = 0.33 ± 0.07 μM, K_d^{ML1} = 41 ± 3 μM, and K_d^{ML2} = 4.5 ± 0.6 μM. In a separate experiment EDANS did not bind to IgE^{DNP} over this concentration range (Figure S1).

(B) Effective inhibitory concentrations of monovalent NF (ML1: ○) and HBL2 (■) were compared in an ELISA assay. BSA conjugated nitrofuran was adsorbed onto the surface of a 96-well plate and increasing concentrations of either HBL2 or ML1 were incubated with IgE^{DNP} antibody prior to the addition to the wells. Inhibition was measured by monitoring the activity of HRP conjugated to a secondary antibody (anti-mouse IgE from goat). IC_{50}^{HBL2} = 0.45 ± 0.05 μM and the IC_{50}^{ML1} = 55 ± 5 μM. The error bars are standard deviations from at least triplicate measurements.

that of monovalent NF (ML1), and a 14-fold enhancement over that of monovalent IBA (ML2). Therefore, we predicted that HBL2 would be the most potent heterobivalent ligand in the inhibition studies.

Heterobivalent Ligands Competitively Inhibit Allergen Binding to IgE Antibody

Allergic reactions are elicited when a multivalent allergen mediates clustering of the FcεRI-bound IgE molecules on the surface of mast cells. To simulate binding of multivalent allergens to IgEs in our experimental system, we synthesized multivalent bovine serum albumin (BSA) NF-BSA in order to mimic allergens. Mass spectrometric analysis showed an average of 17 NF molecules per BSA in NF-BSA conjugates (see Experimental Procedures). We then used a competitive binding enzyme-linked immunosorbent assay (ELISA) to evaluate the efficacy of the heterobivalent ligand HBL2 in inhibiting binding of NF-BSA to IgE^{DNP}. For this purpose, we incubated IgE^{DNP} with increasing concentrations of HBL2 in a 96-well plate coated with NF-BSA until equilibrium was reached. According to our results, HBL2 inhibited the binding of IgE^{DNP} to NF-BSA with an IC_{50} of 0.45 ± 0.05 μM, whereas 55 ± 5 μM of monomeric NF (ML1) was required to achieve 50% inhibition (Figure 3B). In a similar set of experiments performed using the nucleotide analog, IBA, we did not observe any inhibition of NF-BSA binding to the IgE^{DNP}. These results mirrored the findings of the thermodynamic binding constants where HBL2 had greater than two orders of magnitude higher binding affinity for IgE^{DNP} over that of monovalent NF.

Heterobivalent Ligands Effectively Inhibit Mast Cell Degranulation

To assess the potential of HBL2 to inhibit the degranulation response, we used a well-established rat basophilic leukemia (RBL) cell model system (Blank and Rivera, 2006; Posner et al., 2002). These cells have FcεRI receptors on their surfaces that have a high affinity for IgE^{DNP}. It has been previously shown that aggregation of IgE^{DNP} antibodies bound to the FcεRI receptors on RBL cells by DNP-BSA results in a degranulation response with a mechanism similar to degranulation of mast-cells. To adapt the RBL cell model system for our purpose, we optimized the system to achieve a degranulation response by NF-BSA. We first incubated RBL cells with monoclonal mouse IgE^{DNP} to allow the antibody to bind to FcεRI on cell surfaces. Cells were then exposed to NF-BSA in increasing concentrations to crosslink the surface bound IgE^{DNP} antibodies, which in turn stimulate degranulation. We determined that >90% degranulation was achieved at 100 μg/ml NF-BSA, with an EC_{50} of ~50 μg/ml (Figure 4A). Next, to evaluate the inhibitory effect of heterobivalent ligands, we co-incubated RBL cells with NF-BSA and increasing concentrations of HBL2. As can be seen in Figure 4B, HBL2 significantly inhibited the degranulation response induced by NF-BSA, with an IC_{50} of 15 ± 2 μM. As expected the IC_{50} is higher than the K_d because only between 1%–10% of the FcεRI need to be cross linked to initiate degranulation (Holowka and Baird, 1996). We did not detect any inhibition by the monovalent NF at the concentrations tested (Figure 4B), highlighting the remarkable enhancement obtained in the binding affinity to IgE antibody by the heterobivalent ligand. Our control experiments established that HBL2 did not have any cytotoxic effects on the RBL cells, showing that the inhibition of degranulation was by blocking RBL activation and

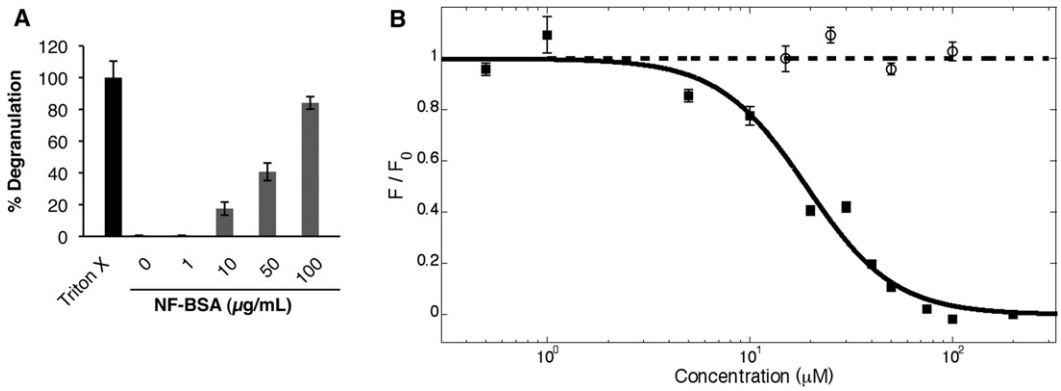

Figure 4. HBL2 Successfully Inhibits Mast Cell Degranulation

(A) Dose response of RBL mast cell degranulation in response to increasing concentrations of NF-BSA. Triton X (1%) was used to normalize the percent degranulation in response to NF-BSA.

(B) Inhibitory potentials of monovalent NF (ML1: ○) and HBL2 (■) were compared in a cellular assay by measuring the activity of β-hexoamidase, an enzyme released during RBL degranulation (Blank and Rivera, 2006). Cells were first treated with saturating concentrations of IgE^{DNP}, and were then activated by NF-BSA. The IC_{50} of HBL2 was determined to be 15 ± 2 μM and no inhibition was observed over this range with ML1. In separate experiments IBA did not inhibit degranulation (Figure S2) and the necessity of the antigen binding moiety was demonstrated (Figure S3). The error bars are standard deviations from at least triplicate measurements.

not due to cytotoxic effects. Furthermore, we synthesized and tested a HBL molecule where the IBA moiety on HBL2 was replaced with dansyl, a structurally similar molecule to IBA but does not bind to the nucleotide binding site. In vitro cellular assays established that this test molecule did not inhibit degranulation (Figure S2). We also tested HBL2 for its potential to inhibit degranulation in a dansyl allergy system, where anti-dansyl IgE (IgE^{Dansyl}) was bound to mast cell FcεRIs, and dansyl-BSA was used as the synthetic allergen. As expected, HBL2 did not inhibit degranulation with this system (Figure S3). Together these control experiments illustrate that bivalent binding of the HBL molecules was indeed the only mechanism by which RBL degranulation was inhibited.

Five more HBL molecules were assessed for their inhibitory potential in RBL degranulation assays. HBL1 and HBL3 showed similar inhibitory effects as HBL2, whereas HBL4 and HBL5 did not have any inhibitory effect (Figure S4). These results were in agreement with measured affinities of these HBLs for IgE^{DNP} and confirmed our prediction that higher avidity would directly correlate with better inhibitory effect.

DISCUSSION

The described studies represent part of our continuing effort to develop heterobivalent ligands that selectively bind to target IgE antibodies with high avidity to competitively inhibit allergen binding, and thereby inhibiting allergic reaction. Inhibition of allergic response using monovalent haptens has not been successful as the affinity of the monovalent hapten falls short in comparison to the avidity of the multivalent allergen. Here, we employ a novel approach, in order to increase avidity (rather than affinity) in the design of heterobivalent ligands that competitively bind to IgE^{DNP} with high specificity and avidity.

Multivalent interactions provide enhanced binding avidity as a result of increased effective molarity. Because the binding components are linked to each other, the initial binding event brings all the other interacting components into proximity; hence the penalty for the translational entropy is prepaid by conjugating binding entities to each other. We calculated the effective molarity for the binding of the hapten component of HBL2 using the equilibrium scheme described in Figure 5, and Equations 1 and 2 below:

$$K_d^{Obs} = K_d^{Ant} \times J^{Nuc} = K_d^{Nuc} \times K^{Ant} \quad (1)$$

and

$$C_{eff} = K_d^{Ant} \times J^{Ant}. \quad (2)$$

We determined that C_{eff} for the NF binding in HBL2 was 562 μM. Hence to compete off half of HBL2 from binding to IgE^{DNP}, this is the necessary concentration of monovalent NF that is needed.

In order to better understand the effects of linker length on binding, we started out by testing ethylene glycol linkers with various lengths. Ethylene glycol (EG) polymers are hydrophilic, flexible, and do not form specific interactions with proteins (Delgado et al., 1992; Harris and Chess, 2003; Roberts et al., 2002). The first four heterobivalent ligands we synthesized had varying lengths of EG linkers: HBL1 (EG_5) was 2.5 nm, HBL2 (EG_6) was 2.9 nm, HBL3 (EG_8) was 3.4 nm long, and HBL4 (EG_{24}) was 9.2 nm long. Analysis of the relative binding constants provide information about the distance between the binding sites. HBL1 had a K_d of 0.79 ± 0.06 μM, which suggested a weaker binding interaction than HBL2 (K_d = 0.33 ± 0.07 μM). This result suggested that the length of EG_5 linker did not provide the optimal length for binding of both moieties simultaneously. Using the longer linker, EG_8, in HBL3 resulted in a slight weakening of the affinity (K_d = 0.55 ± 0.03 μM) compared to HBL2. The ligand HBL4 with the longest linker, EG_{24}, had even weaker binding affinity (0.96 ± 0.05 μM). The decrease in the affinities of HBL3 and HBL4 is due to the increased conformational entropy of the heterobivalent molecules as a result of the increase in the

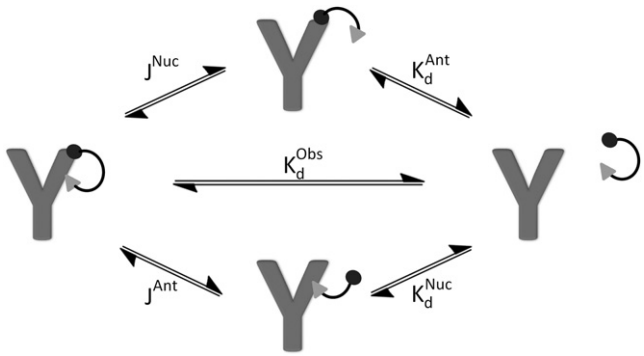

Figure 5. Bivalent Binding Enhances Ligand Avidity

Reaction equilibria for the binding of heterobivalent ligands to IgE^{DNP}. The K_d^{Obs} are the reported binding constants for the heterobivalent ligands listed in Table 1. K_d^{Ant} is the dissociation constant of monovalent hapten (ML1), and K_d^{Nuc} is the dissociation constant of monovalent nucleotide analog (ML2). J^{Ant} and J^{Nuc} are the unitless intramolecular binding constants for antigen and nucleotide analog respectively. We calculated the values for these constants to be J^{Nuc} = 0.008 and J^{Ant} = 0.073 for HBL2 binding to IgE^{DNP}.

linker length (Kane, 2010). According to the results of the set of ethylene glycol linkers, we conclude that the optimal linker length is ~3 nm.

Next, we tested the effect of linker hydrophobicity on the overall avidity. Because both the nucleotide and the antigen binding sites are sandwiched between the heavy and light chains of the Fab region with several hydrophobic contacts, we expected that a more hydrophobic linker would interact favorably with the antibody surface and increase the binding thermodynamics of the ligands. The results, however, were just the opposite of our predictions. Heterobivalent molecules HBL5 and HBL6, with flexible hydrophobic linkers of different lengths had binding constants of 30 ± 3 μM and 15 ± 1 μM respectively. The weaker binding ligand HBL5 had a shorter linker length, suggesting that the optimal linker length for this linker needed to be longer than 2.67 nm. Nevertheless, even ligand HBL6, the more favorable of the two, had a 50-fold weaker binding affinity compared to HBL2. In fact, this binding affinity is still weaker than the monovalent IBA (ML2), which had a K_d = 4.5 ± 0.6 μM. We hypothesize that the reason for this weakened affinity is due to unfavorable interactions between the linker and the antibody surface, or possibly that the linker might be folding onto itself resulting in the weakened binding to the antibody.

In order to investigate the effects of linker flexibility on binding affinity, we synthesized another series of hydrophobic compounds with increasing rigidity, molecules HBL7, HBL8, HBL9, and HBL10. Hypothetically, increasing rigidity of the linker should result in decreased penalty for conformational entropy upon binding, with an effect similar to the observed decrease in affinity with increased ethylene glycol linker length. Therefore, the more rigid the linker, the more favorable the interaction should be. The results of the binding constants for this series, however, show just the opposite trend. This is possibly a result of two effects: (1) the rigid linker monomer we used was highly hydrophobic, and as we learned from the earlier series of compounds, increased hydrophobicity did not result in a favorable binding interaction; and (2) the six-membered cyclic ring structure was possibly too rigid to accommodate the binding of both groups simultaneously in the correct geometry. The binding affinities of the compounds in this series (HBL7-10) varied between 15 ± 1 μM to 1.6 ± 0.2 μM, about an order of magnitude separating the best binding (HBL7; K_d = 1.6 ± 0.2 μM) and the worst binding (HBL10; K_d = 15 ± 1 μM) ligands. HBL7, however, still had weaker affinity than ligand HBL2, which again suggested that the surface of the antibody did not favor hydrophobic interactions with the linker moieties. Results of the thermodynamic analysis of the heterobivalent molecules established that ligand HBL2 had the highest potential to successfully inhibit antibody/allergen interaction in competitive binding experiments.

In summary, increasing the avidity of the hapten by conjugating a nucleotide binding site targeting moiety with an appropriate linker provided very favorable results for inhibiting the IgE/allergen interaction. In the ELISA binding assay, heterobivalent ligand HBL2 had an IC_{50} of 0.45 ± 0.05 μM for inhibiting the binding of the allergen mimic (NF-BSA) to IgE^{DNP}, whereas the IC_{50} of monovalent NF was 55 ± 5 μM (Figure 3B). More remarkably, in the in vitro cellular degranulation assay, we determined that HBL2 had an IC_{50} of 15 ± 2 μM, whereas we did not observe any inhibition by the monovalent hapten even at the elevated concentrations in the titration (Figure 4B). We believe that the relative weak affinity of the hapten (K_d = 41 ± 3 μM) had a negative effect on the increase in avidity, as, in principle, a heterobivalent molecule synthesized with a higher affinity hapten would have yielded an enhancement in binding higher than that was observed in the described system.

We establish in this study a formerly unexplored practical use for the unconventional nucleotide binding site on the immunoglobulins that paves the way for a molecular engineering approach to selectively inhibit allergic response. The potential for using heterobivalent ligand design in allergic response inhibition will increase as knowledge of immune epitopes increases and the significance of certain epitopes in specific allergies becomes clearer. Meanwhile, this approach of targeted inhibition is readily applicable to allergies where the allergen is a small well-defined molecule such as in allergies to β-lactam antibiotics or any in the class of sulfonamide drugs. Specifically, our technology has the potential to greatly increase the effectiveness of haptenic derivatives of penicillin as it has been shown that such molecules are able to inhibit IgE-penicillin interaction albeit in very high concentrations (Fernandez et al., 1995; Zhao et al., 2001). Furthermore, our approach has broad application in inhibiting food allergies, environmental allergies, and asthmas. A critical component for the success of this approach in such allergies is the identification of allergy epitopes. Currently, there is significant effort for the identification and characterization of various epitopes in the allergy field; several research groups have identified some of the most frequent reactive sites on common allergens using high through-put screening techniques such as phage display, peptide microarrays, and molecular modeling (Cerecedo et al., 2008; Pacios et al., 2008; Riemer et al., 2004; Rougé et al., 2009; Tordesillas et al., 2010). Increasing amounts of data are becoming available due to the technological advances in epitope mapping techniques and establishment of centralized databases such as Immune Epitope Database (Vita et al., 2010). Identification of these sites provides a starting point for the design of heterobivalent ligands that can be used in specific inhibition of a particular allergy.

SIGNIFICANCE

One of the challenges in the current therapies used to treat adverse immunological responses such as allergies is the nonspecific suppression of immune system that puts patients at increased risk for infections and even development of cancers. This underlines the need to develop more specific treatments for such adverse immunological responses without the overall suppression of the immune system. Here, by using a variant of an IgE/DNP model system, we demonstrate the proof of principle studies of a new approach that has the potential to respond to this need by selectively inhibiting mast cell degranulation. Specifically, we designed heterobivalent ligands that simultaneously bind to two nearby sites located on the Fab domains of IgE molecules—the antigen binding and the nucleotide binding sites. These dual targeting molecules have enhanced avidity and selectivity for a target IgE antibody. The heterobivalent ligands showed up to 124-fold higher affinity for the specific IgE compared to monovalent hapten, and successfully inhibited mast cell degranulation whereas the monovalent hapten did not show any inhibition even at elevated concentrations. The described method of targeted inhibition can have broad applications in inhibiting food allergies, environmental allergies, and asthmas where the allergy epitopes are known. As an example, the design can be applied to inhibit allergies caused by β-lactam antibiotics or any in the class of sulfonamide drugs where the allergen is a well-defined small molecule. Finally, this study establishes, for the first time, a new practical use for the previously neglected unconventional nucleotide binding site found on the Fab domain of immunoglobulins.

EXPERIMENTAL PROCEDURES

Materials

We purchased *N*-Fmoc-amido-dPEG$_8$-acid and *N*-Fmoc-amido-dPEG$_{24}$-acid from Quanta BioDesign, Fmoc-NH-(PEG)$_4$-COOH, Fmoc-NH-(PEG)$_5$-COOH, *N*-Fmoc-amino acids, Fmoc-lys(ivDde)-OH, NovaPEG Rink Amide resin, 2-(1H-benzotriazole-1-yl)-1,1,3,3-tetramethyluronium hexafluorophosphate (HBTU), and BSA from EMD Biosciences. Indole-3-butyric acid, 5-nitro-2-furoic acid, *N*,*N*-diisopropylethylamine (DIEA), N-(3-dimethylaminopropyl)-N′-ethylcarbodiimide (EDC), trifluoroacetic acid (TFA), and piperidine from Sigma and *N*,*N*-dimethylformamide (DMF) (>99.8%) were purchased from Thermo Fisher. IgE^{DNP} was a monoclonal IgE isolated from ascites, and was purified using a trinitrophenyl-lysine affinity column.

Design of the Heterobivalent Ligand

The heterobivalent ligand has three important components that contribute to binding avidity: (1) the hapten, (2) the nucleotide analog, and (3) a linker connecting these two moieties. The hapten and the nucleotide analog were chosen based on the criteria described above. Next we screened for the linker with optimal properties. Three properties are important when choosing the appropriate linker: length, flexibility, and chemistry (hydrophobicity, polarity, charge, and H-bonding capability). Upon analyzing the crystal-structure of the Fab domain of an IgE^{DNP} antibody (Protein Data Bank [PDB] 2r56), the shortest distance between the antigen-binding and the nucleotide-binding sites was found to be >2.5 nm. We took this distance as the minimum linker length necessary to span the two sites. Flexibility is another important parameter for the linker such that it can conform to the surface topology of the IgE^{DNP} and not cause steric impediments to binding. The chemical properties of the linker are yet another set of important parameters: favorable interactions between the linker and the surface of the IgE that span the antigen-binding site and the nucleotide binding site would be manifested as an increased overall avidity of the heterobivalent ligand to the IgE. Therefore, we screened multiple linkers experimentally to determine their effect on the avidity of the heterobivalent ligands to IgE^{DNP}. Each heterobivalent ligand linker has unique properties and the same pair of hapten and nucleotide analog attached allowing us to decipher the optimal properties for the linker yielding the heterobivalent ligand with the best binding avidity.

Synthesis of Heterobivalent Ligands

The heterobivalent ligands were synthesized using Fmoc chemistry on a solid support. Residues were activated with HBTU and DIEA in DMF for 3 min and coupling completion was monitored with Keiser tests. The Fmoc protected residues were deprotected using 3 × 20% piperidine in DMF for 3 min. After the addition of indole-3-butyric acid the ivDde protecting group was selectively removed from the lysine residue using 3 × 2% hydrazine in DMF for 3 min providing a free amine for the addition of 5-nitro-2-furoic acid. The ligands were cleaved from the solid support using 2 × 92/4/4 TFA/H_2O/TIS for 30 min. We purified the heterobivalent ligands using RP-HPLC on an Agilent 1200 series system with a semi-preparative Zorbax C18 column (9.4 mm × 250 mm), using linear solvent gradients of 2.5% min^{-1} increments in acetonitrile concentration at 4.0 ml/min flow rate. We monitored the column eluent with a diode array detector allowing a spectrum from 200 to 400 nm to be analyzed. The purified product was characterized using a Bruker micrOTOF II mass spectrometer and a Varian Unity*Plus* 300 NMR (Supplemental Information). The purity of all synthesized ligands was estimated to be >97% by an analytical injection using the above described HPLC with a Zorbax C18 analytical column (4.6 mm × 150 mm). The calculated molecular mass of ML1 ($C_{24}H_{41}N_5O_{11}$) was 575.3 Da; found 576.3 Da (with sodium adduct at 598.3 Da), the calculated molecular mass of ML2 ($C_{40}H_{53}N_{10}O_{10}S_1$) was 865.4 Da; found 866.4 Da (with sodium adduct at 888.4 Da), the calculated molecular mass of HBL1 ($C_{42}H_{62}N_6O_8$) was 760.4 Da; found 761.4 Da (with sodium adduct at 783.4 Da), the calculated molecular mass of HBL2 ($C_{38}H_{56}N_6O_{13}$) was 804.4 Da; found 805.4 Da (with sodium adduct at 827.4 Da), the calculated molecular mass of HBL3 ($C_{42}H_{64}N_6O_{15}$) was 892.4 Da; found 893.4 Da (with sodium adduct at 915.4 Da), the calculated molecular mass of HBL5 ($C_{41}H_{62}N_{10}O_9$) was 838.5 Da; found 839.5 Da (with sodium adduct at 861.5 Da), the calculated molecular mass of HBL6 ($C_{47}H_{74}N_{12}O_{10}$) was 966.6 Da; found 967.6 (with sodium adduct at 989.6 Da), the calculated molecular mass of HBL7 ($C_{43}H_{62}N_8O_{10}$) was 898.4 Da; found 899.4 Da (with sodium adduct at 921.4), the calculated molecular mass of HBL8 ($C_{51}H_{74}N_{10}O_{15}$) was 1066.5 Da; found 1067.5 Da (with sodium adduct at 1089.5 Da), the calculated molecular mass of HBL9 ($C_{49}H_{71}N_9O_{14}$) was 1009.5 Da; found 1010.5 Da (with sodium adduct at 1032.5 Da), the calculated molecular mass of HBL10 ($C_{69}H_{105}N_{11}O_{20}$) was 1407.7 Da; found 1408.7 (with sodium adduct at 1430.7 Da).

Synthesis of Conjugated BSA

BSA (10 mg) was dissolved in 1 ml of MES buffer (0.1 M pH 4.7), 4 mg of 5-nitro-2-furoic acid was dissolved in 1 ml of MES buffer, EDC (10 mg) was dissolved in 100 μL of MES buffer and immediately added to a solution of 200 μL of BSA, and 500 μL of 5-nitro-2-furoic acid. Fresh EDC was added every 45 min until the desired number of nitrofurans were conjugated to BSA. Conjugation was monitored using SE-HPLC on an Agilent 1200 series system with a Tosoh Bioscience TSKgel Super SW3000 column (4.6 mm × 300 mm) at 0.25 ml/min PBS (pH 6.8) and characterized using a Bruker AutoFlex MALDI TOF/TOF. The conjugated BSA was purified using a Corning Spin-X UF concentrator with a 30 kDa membrane. The purity of NF-BSA (elution time 10.7 min) was estimated to be >95% using the SE-HPLC method described earlier where the only contaminant detected was unreacted excess NF at <5% (elution time 15.2 min). The molecular mass of unmodified BSA was 66869.4 Da (with double charged peak at 33492.9 m/z), and the NF-BSA had a molecular mass of 68940.5 Da (with double charged peak at 34800.2 m/z) indicating an average addition of ~17 NF molecules per BSA. Additionally the purified NF-BSA was lyophilized allowing us to determine the amount of protein by mass and concentration of NF by absorbance. The number of NF/BSA determined using this method was in agreement with the number of NF/BSA determined by mass spectometry.

Fluorescence Quenching Assay

NF has a maximum absorbance at 314 nm, whereas tryptophan fluorescence is at 335 nm. The overlap in NF absorbance and tryptophan fluorescence

provided a straightforward spectroscopic method to directly measure the extent of association between the heterobivalent molecules and the IgE^{DNP}. Upon heterobivalent molecule binding to the IgE^{DNP}, the fluorescence from the IgE^{DNP} tryptophan residues were quenched by the nitrofuran. To determine the binding constants of nucleotide analogs, we conjugated the molecule to EDANS (max absorbance 335 nm), which also quenches the fluorescence of tryptophan residues. The binding constant (K'_d) can be calculated from Equation 3,

$$K'_d = \frac{[IgE][L]}{[IgE\ L]}, \quad (3)$$

where L is the ligand. When the starting IgE^{DNP} concentration is significantly below the value of K_d ($[IgE^{DNP}] < K_d$), then upon binding to the antibody the free ligand concentration in solution does not change. By dividing the measured fluorescence (F) to the fluorescence in the absence of ligand (F_o), the effect of quenching can be normalized. Hence, K'_d becomes equal to concentration of L at the deflection point of the titration sigmoid for (F/F_o) versus [L]. Therefore, rearranging Equation 3 yields Equation 4. K_d can be calculated from Equation 4,

$$\frac{F}{F_o} = 1 - \left(\frac{[L]}{([L] + K_d)}\right). \quad (4)$$

We normalized the measured fluorescence using Equation 5,

$$\frac{F}{F_o} = \frac{[F_{\alpha,\ell,PBS} - F_{\ell,PBS}]}{[F_{\alpha,PBS} - F_{PBS}]}, \quad (5)$$

where F denotes the measured fluorescence at 335 nm, and the subscripts indicates the compounds that are also present in the sample, where α is IgE^{DNP}, ℓ is the ligand being analyzed for binding, and PBS is the buffer. At high concentrations of ligand the fluorescence of the tryptophan residues in the antibody can be quenched by ligands that are in proximity to the IgE although they may not be forming any interactions with it. This is due to fluorescence quenching efficiency being based on proximity of the donor molecule to the acceptor molecule. As the concentration of the ligand increases the statistical probability of finding a quencher molecule close to the donor significantly increases. To account for the random quenching an extra term was added to Equation 5 yielding Equation 6,

$$\frac{F}{F_o} = \frac{[F_{\alpha,\ell,PBS} - F_{\ell,PBS}]}{[F_{\alpha,PBS} - F_{PBS}]} + \left\{\ell - \frac{[F_{w,\ell,PBS} - F_{\ell,PBS}]}{[F_{w,PBS} - F_{PBS}]}\right\}, \quad (6)$$

where the subscript w is free tryptophan. The ligands analyzed do not bind to free tryptophan so any observed quenching of free tryptophan fluorescence is due to the ligand being in close proximity to tryptophan (effect only observed at high ligand concentrations). Because there are two antigen/nucleotide binding sites per antibody, the binding entity (e.g., hapten, nucleotide, or HBL) will be distributed evenly throughout all available sites. At ligand concentrations equal to the observed binding constant K'_d, there will be a statistical distribution of three antibody/binder complex subpopulations: 50% of the complex is going to have be one antibody with one binder, 25% will have two binders (both Fab arms occupied), and 25% will not have any binder at all. Fluorescence quenching does not distinguish between singly bound and doubly bound antibody/binder complexes, and because during titration 25% of the antibody is found uncomplexed, the observed binding constant (K'_d) will be higher (suggesting weaker affinity) than the real binding constant (K_d) by a statistical factor that reflects the distribution of the ligand between the subpopulations. Therefore, the actual monovalent binding constant (K_d) is equal to three-fourths of the observed binding constant K'_d as determined by fluorescence quenching. Accordingly, actual monovalent binding constant K_d can be calculated as

$$K_d = 3/4K'_d. \quad (7)$$

During experiment, IgE^{DNP} was diluted into PBS (pH 7.4) at a concentration of 100 nM. IgE^{DNP} solution (100 μL) was added to the wells of a 96-well, low protein binding, plate. Increasing amounts of the heterobivalent ligand were added to the wells and tryptophan fluorescence of IgE^{DNP} was monitored (excitation, 280 nm; emission, 335 nm). All fluorescence-binding experiments were done at least in triplicates.

ELISA

The wells of a 96-well ELISA plate were incubated with NF-BSA conjugate to adsorb it onto the surface. The ligand to be assayed was incubated with IgE^{DNP} for 30 min prior to being added to the wells. After treating the plate with the ligand to be assayed and washing, we incubated the plate with a secondary antibody (anti-mouse IgE from goat) conjugated to horseradish peroxidase (HRP) purchased from AbD Serotec. After washing, we treated the wells with Amplex Red, and monitored the HRP-catalyzed hydrolysis of this substrate using fluorescence (excitation, 545 nm; emission, 590 nm). All ELISA experiments were done at least in triplicates.

RBL Degranulation Assay

RBL cells and IgE^{DNP} were kindly provided by Dr. Wilson (University of New Mexico). RBL cells were maintained as described previously (Andrews et al., 2007). For the degranulation assay, cells were plated at 0.5×10^6 cells/ml in a 96-well plate, and were incubated overnight with 1 μg/ml IgE^{DNP} to saturate the receptors. Cells were washed immediately before experiments and were stimulated with the indicated concentrations of NF-BSA. Degranulation was detected as described earlier (Holowka and Baird, 1996). Triton (1%) was used to determine the maximum response. For inhibition experiments, cells were co-incubated with increasing concentrations of the heterobivalent ligand. Monovalent IBA and monovalent NF were used as controls. All degranulation assays were done at least in triplicates.

Computational Screening for Nucleotide Analogs

Small molecule docking was used to predict the binding modes and relative affinities of 15 nucleotide analog candidates. We obtained 2D structures of the ligands (in SDF file format) from the PubChem database (http://pubchem.ncbi.nlm.nih.gov/). The QuacPac and Omega programs provided by OpenEye Scientific Software (http://www.eyesopen.com/) were used to enumerate the potential tautomers, protonation states, and 3D conformations of each compound. QuacPac was also used to assign AM1-BCC partial charges to each of the ligands. The antibody structure (PDB code 1MRC) was prepared for docking using the MOE program (http://www.chemcomp.com/) to remove crystallographic waters from the structure, and to assign partial electrostatic charges from the AMBER99 force field. We used the FRED program from OpenEye to perform the docking; a docking grid that enclosed the desired binding site with 4.0 Å margins was constructed. We performed exhaustive docking of the compounds using the ZapBind Poisson-Boltzmann implicit solvation scoring function. The top-scoring binding pose of each compound was saved to the results file, and the list of compounds was prioritized by the ZapBind score values.

SUPPLEMENTAL INFORMATION

Supplemental Information includes fourteen figures and can be found with this article online at doi:10.1016/j.chembiol.2011.06.012.

ACKNOWLEDGMENTS

We thank Dr. Wilson (University of New Mexico) for generously providing us with IgE^{DNP} and the RBL cells. We thank Dr. Bill Boggess at the Mass Spectrometry and Proteomics Facility in the University of Notre Dame for his help and insightful discussions. We also thank OpenEye Scientific Software (Santa Fe, NM; http://www.eyesopen.com/), and the Chemical Computing Group (Montreal, Quebec, Canada; http://www.chemcomp.com/) for providing computational chemistry software used in this study.

Received: February 12, 2011
Revised: May 10, 2011
Accepted: June 13, 2011
Published: September 22, 2011

REFERENCES

Andrews, N., Lidke, K.A., Hsieh, G., Wilson, B.S., Oliver, J.M., and Lidke, D.S. (2007). High affinity IgE receptor diffusional dynamics measured by single quantum dot tracking in resting and activated cells. FASEB J. *21*, A184.

Baird, E.J., Holowka, D., Coates, G.W., and Baird, B. (2003). Highly effective poly(ethylene glycol) architectures for specific inhibition of immune receptor activation. Biochemistry *42*, 12739–12748.

Bilgiçer, B., Moustakas, D.T., and Whitesides, G.M. (2007). A synthetic trivalent hapten that aggregates anti-2,4-DNP IgG into bicyclic trimers. J. Am. Chem. Soc. *129*, 3722–3728.

Bilgiçer, B., Thomas, S.W., 3rd, Shaw, B.F., Kaufman, G.K., Krishnamurthy, V.M., Estroff, L.A., Yang, J., and Whitesides, G.M. (2009). A non-chromatographic method for the purification of a bivalently active monoclonal IgG antibody from biological fluids. J. Am. Chem. Soc. *131*, 9361–9367.

Blank, U., and Rivera, J. (2006). Assays for regulated exocytosis of mast cell granules. Curr. Protoc. Cell Biol., Chapter 15, Unit 15.11.

Carlson, C.B., Mowery, P., Owen, R.M., Dykhuizen, E.C., and Kiessling, L.L. (2007). Selective tumor cell targeting using low-affinity, multivalent interactions. ACS Chem. Biol. *2*, 119–127.

Cerecedo, I., Zamora, J., Shreffler, W.G., Lin, J., Bardina, L., Dieguez, M.C., Wang, J., Muriel, A., de la Hoz, B., and Sampson, H.A. (2008). Mapping of the IgE and IgG4 sequential epitopes of milk allergens with a peptide microarray-based immunoassay. J. Allergy Clin. Immunol. *122*, 589–594.

Delgado, C., Francis, G.E., and Fisher, D. (1992). The uses and properties of PEG-linked proteins. Crit. Rev. Ther. Drug Carrier Syst. *9*, 249–304.

Fernandez, M., Warbrick, E.V., Blanca, M., and Coleman, J.W. (1995). Activation and hapten inhibition of mast cells sensitized with monoclonal IgE anti-penicillin antibodies: evidence for two-site recognition of the penicillin derived determinant. Eur. J. Immunol. *25*, 2486–2491.

Galli, S.J., Tsai, M., and Piliponsky, A.M. (2008). The development of allergic inflammation. Nature *454*, 445–454.

Guéant, J.L., Mata, E., Namour, F., Romano, A., Aimone-Gastin, I., Kanny, G., Moneret-Vautrin, D.A., and Laxenaire, M.C. (1999). Criteria of evaluation and of interpretation of Sepharose drug IgE-RIA to anaesthetic drugs. Allergy *54* (*Suppl 58*), 17–22.

Harris, J.M., and Chess, R.B. (2003). Effect of pegylation on pharmaceuticals. Nat. Rev. Drug Discov. *2*, 214–221.

Holowka, D., and Baird, B. (1996). Antigen-mediated IGE receptor aggregation and signaling: a window on cell surface structure and dynamics. Annu. Rev. Biophys. Biomol. Struct. *25*, 79–112.

James, L.C., Roversi, P., and Tawfik, D.S. (2003). Antibody multispecificity mediated by conformational diversity. Science *299*, 1362–1367.

Kane, P.M., Holowka, D., and Baird, B. (1988). Cross-linking of IgE-receptor complexes by rigid bivalent antigens greater than 200 A in length triggers cellular degranulation. J. Cell Biol. *107*, 969–980.

Kane, R.S. (2010). Thermodynamics of multivalent interactions: influence of the linker. Langmuir *26*, 8636–8640.

Kane, R.S. (2006). Polyvalency: recent developments and new opportunities for chemical engineers. AIChE J. *52*, 3638–3644.

Kiessling, L.L., Gestwicki, J.E., and Strong, L.E. (2006). Synthetic multivalent ligands as probes of signal transduction. Angew. Chem. Int. Ed. Engl. *45*, 2348–2368.

Kitov, P.I., Sadowska, J.M., Mulvey, G., Armstrong, G.D., Ling, H., Pannu, N.S., Read, R.J., and Bundle, D.R. (2000). Shiga-like toxins are neutralized by tailored multivalent carbohydrate ligands. Nature *403*, 669–672.

Mammen, M., Choi, S.K., and Whitesides, G.M. (1998). Polyvalent interactions in biological systems: Implications for design and use of multivalent ligands and inhibitors. Angew. Chem. Int. Ed. *37*, 2754–2794.

Mertes, P.M., Aimone-Gastin, I., Guéant-Rodriguez, R.M., Mouton-Faivre, C., Audibert, G., O'Brien, J., Frendt, D., Brezeanu, M., Bouaziz, H., and Guéant, J.L. (2008). Hypersensitivity reactions to neuromuscular blocking agents. Curr. Pharm. Des. *14*, 2809–2825.

Metzger, H. (1992). Transmembrane signaling: the joy of aggregation. J. Immunol. *149*, 1477–1487.

Oliver, J.M., Burg, D.L., Wilson, B.S., McLaughlin, J.L., and Geahlen, R.L. (1994). Inhibition of mast cell Fc epsilon R1-mediated signaling and effector function by the Syk-selective inhibitor, piceatannol. J. Biol. Chem. *269*, 29697–29703.

Pacios, L.F., Tordesillas, L., Cuesta-Herranz, J., Compes, E., Sánchez-Monge, R., Palacín, A., Salcedo, G., and Díaz-Perales, A. (2008). Mimotope mapping as a complementary strategy to define allergen IgE-epitopes: peach Pru p 3 allergen as a model. Mol. Immunol. *45*, 2269–2276.

Posner, R.G., Savage, P.B., Peters, A.S., Macias, A., DelGado, J., Zwartz, G., Sklar, L.A., and Hlavacek, W.S. (2002). A quantitative approach for studying IgE-FcepsilonRI aggregation. Mol. Immunol. *38*, 1221–1228.

Rajagopalan, K., Pavlinkova, G., Levy, S., Pokkuluri, P.R., Schiffer, M., Haley, B.E., and Kohler, H. (1996). Novel unconventional binding site in the variable region of immunoglobulins. Proc. Natl. Acad. Sci. USA *93*, 6019–6024.

Rao, J.H., Lahiri, J., Weis, R.M., and Whitesides, G.M. (2000). Design, synthesis, and characterization of a high-affinity trivalent system derived from vancomycin and L-Lys-D-Ala-D-Ala. J. Am. Chem. Soc. *122*, 2698–2710.

Richter, W., Hedin, H., Kraft, D., and Messmer, K. (1981). [Anaphylactoid reactions after dextran. I. Immunology of the pathomechanism and the hapten inhibition]. Beitr. Infusionther. Klin. Ernahr. *8*, 54–65.

Riemer, A., Scheiner, O., and Jensen-Jarolim, E. (2004). Allergen mimotopes. Methods *32*, 321–327.

Roberts, M.J., Bentley, M.D., and Harris, J.M. (2002). Chemistry for peptide and protein PEGylation. Adv. Drug Deliv. Rev. *54*, 459–476.

Romano, A., and Ventura, M. (2008). Advances in diagnosing drug hypersensitivity reactions. Curr. Pharm. Des. *14*, 2767–2769.

Rougé, P., Culerrier, R., Sabatier, V., Granier, C., Rancé, F., and Barre, A. (2009). Mapping and conformational analysis of IgE-binding epitopic regions on the molecular surface of the major Ara h 3 legumin allergen of peanut (Arachis hypogaea). Mol. Immunol. *46*, 1067–1075.

Salvin, S.B. (1971). Roles of haptens and carriers in delayed allergies. Adv. Biol. Skin *11*, 95–101.

Tong, G.J., Hsiao, S.C., Carrico, Z.M., and Francis, M.B. (2009). Viral capsid DNA aptamer conjugates as multivalent cell-targeting vehicles. J. Am. Chem. Soc. *131*, 11174–11178.

Tordesillas, L., Pacios, L.F., Palacín, A., Cuesta-Herranz, J., Madero, M., and Díaz-Perales, A. (2010). Characterization of IgE epitopes of Cuc m 2, the major melon allergen, and their role in cross-reactivity with pollen profilins. Clin. Exp. Allergy *40*, 174–181.

Turner, H., and Kinet, J.P. (1999). Signalling through the high-affinity IgE receptor Fc epsilonRI. Nature *402* (6760, Suppl), B24–B30.

Vance, D., Shah, M., Joshi, A., and Kane, R.S. (2008). Polyvalency: a promising strategy for drug design. Biotechnol. Bioeng. *101*, 429–434.

Vita, R., Zarebski, L., Greenbaum, J.A., Emami, H., Hoof, I., Salimi, N., Damle, R., Sette, A., and Peters, B. (2010). The immune epitope database 2.0. Nucleic Acids Res. *38* (Database issue), D854–D862.

Wang, J.Q., Chen, X., Zhang, W., Zacharek, S., Chen, Y.S., and Wang, P.G. (2000). Enhanced inhibition of human anti-Gal antibody binding to mammalian cells by synthetic alpha-Gal epitope polymers. J. Am. Chem. Soc. *121*, 8174–8181.

Wieslander, J., Mansson, O., Kallin, E., Gabrielli, A., Nowack, H., and Timpl, R. (1990). Specificity of human-antibodies against Gal-alpha-1-3Gal carbohydrate epitope and distinction from natural antibodies reacting with Gal-alpha-1-2Gal or Gal-alpha-1-4Gal. Glycoconj. J. *7*, 85–100.

Wolfenden, M.L., and Cloninger, M.J. (2005). Mannose/glucose-functionalized dendrimers to investigate the predictable tunability of multivalent interactions. J. Am. Chem. Soc. *127*, 12168–12169.

Yi, H., Rubloff, G.W., and Culver, J.N. (2007). TMV microarrays: hybridization-based assembly of DNA-programmed viral nanotemplates. Langmuir *23*, 2663–2667.

Zhang, Z.S., Liu, J.Y., Verlinde, C.L., Hol, W.G.J., and Fan, E.K. (2004). Large cyclic peptides as cores of multivalent ligands: application to inhibitors of receptor binding by cholera toxin. J. Org. Chem. *69*, 7737–7740.

Zhao, Z.J., Baldo, B.A., Baumgart, K.W., and Mallon, D.F.J. (2001). Fine structural recognition specificities of IgE antibodies distinguishing amoxicilloyl and amoxicillanyl determinants in allergic subjects. J. Mol. Recognit. *14*, 300–307.

